



Published in final edited form as:

*Ultrasound Obstet Gynecol.* 2013 February ; 41(2): 152–161. doi:10.1002/uog.12344.

## Evaluation of cervical stiffness during pregnancy using semiquantitative ultrasound elastography

Edgar Hernandez-Andrade, MD<sup>1,2</sup>, Sonia S Hassan, MD<sup>1,2</sup>, Hyunyoung Ahn, MD, PhD<sup>1,2</sup>, Steven J. Korzeniewski, PhD<sup>1,2</sup>, Lami Yeo, MD<sup>1,2</sup>, Tinnakorn Chaiworapongsa, MD<sup>1,2</sup>, and Roberto Romero, MD, D. Med. Sci<sup>1</sup>

<sup>1</sup>Perinatology Research Branch, NICHD/NIH/DHHS, Bethesda, Maryland and Detroit, Michigan, USA

<sup>2</sup>Department of Obstetrics and Gynecology, Wayne State University School of Medicine, Detroit, Michigan, USA

### Abstract

**Objective**—To evaluate cervical stiffness during pregnancy using ultrasound-derived elastography, a method used to estimate the average tissue displacement (strain) on a defined region of interest when oscillatory compression is applied.

**Methods**—Strain was calculated in two regions of interest, the endocervical canal and the entire cervix, from three anatomical planes of the cervix: mid-sagittal in the plane used for cervical length measurement, and in cross-sectional planes located at the internal and external cervical os. Associations between strain values, method of ascertainment and patient characteristics were assessed using linear mixed models to account for within-subject correlation. Inter-rater agreement in defining the degree of cervical stiffness was evaluated in 120 regions of interest acquired by two operators in 20 patients.

**Results**—A total of 1557 strain estimations were performed in 262 patients at 8-40 weeks of gestation. Adjusting for other sources of variation, 1) cervical tissue strain estimates obtained in the endocervical canal were on average 33% greater than those obtained in the entire cervix; 2) measures obtained in the cross-sectional plane of the external cervical os and sagittal plane were 45% and 13% greater compared to those measured in the cross-sectional plane of the internal cervical os, respectively; 3) mean strain rate was 14% and 5% greater among multiparous women with and without a history of preterm delivery compared to nulliparous women, respectively, and was on average 13% greater among women with a cervical length between 25-30mm compared to those with a cervical length >30mm; and 4) cervical tissue strain was more strongly associated with cervical length than with gestational age.

**Conclusion**—Semiquantitative elastography can be employed to evaluate changes in cervical stiffness during pregnancy.

## Keywords

Cervix; strain; cervical length; transvaginal ultrasound

---

## Introduction

Ultrasound-derived elastography has been successfully applied in the diagnosis and classification of breast<sup>1-4</sup> and thyroid tumors<sup>5,6</sup>, lymph nodes,<sup>7</sup> prostate cancer<sup>8</sup> and diffuse/focal liver disease<sup>9,10</sup>, and has recently been introduced in obstetrics and gynecology<sup>11-18</sup>. Elastography is used to evaluate stiffness and is based on the estimation of displacement of moving tissues when oscillatory pressure is applied<sup>4,19-22</sup>. The method assesses three mechanical properties: 1) stress; 2) strain; and 3) deformation<sup>23</sup>. “Stress” represents the pressure applied per unit area to the structure; pressure produces displacement and changes in the shape of the structure (“deformation, strain”)<sup>24-26</sup>. Stiffness is the resistance of tissues or structures to displacement and deformation, and is inversely related to strain<sup>23</sup>.

Tissue displacement can be estimated using ultrasound (US) by tracking movements among consecutive frames; the average displacement of all structures within a region of interest represents the strain rate<sup>22,24,27-30</sup>. Strain can be displayed by a color code. Conventionally, blue represents stiff tissue, green is indicative of average stiff/soft tissue, and red represents soft tissue. This color code differs across US units and can be modified by the operator<sup>31,32</sup>. In most elastography reports in obstetrics and gynecology, the definition of tissue stiffness/softness relies on this operator-dependent qualitative estimation<sup>11,14,17</sup>. Alternatively, strain can be expressed numerically as the percentage of tissue displacement within a region of interest<sup>15,31</sup>.

In obstetrics, cervical elastography may yield clinically meaningful information, considering that, during normal pregnancy, the uterine cervix undergoes physiological changes in the extracellular matrix in order to reduce stiffness, but increase its tensile properties. These changes are thought to represent cervical adaptation to progressive increases in intrauterine pressure from the growing fetus<sup>33-37</sup>. Elastography can document the degree of cervical stiffness/softness which, in addition to cervical length, might constitute a complementary method to identify cases at risk for preterm delivery. During labor, elastography might provide additional information on the process of cervical effacement to that obtained from digital examination and conventional ultrasound<sup>38-44</sup>. It also may be helpful to assess the likelihood of successful induction of labor.

The aims of this study were to: 1) examine methodological variation in cervical tissue strain estimation; 2) investigate whether patient characteristics modify the relationship between method of measurement and estimated tissue strain; and 3) propose a method for estimating changes in cervical stiffness during pregnancy using ultrasound-derived elastography.

## Materials and Methods

In this cross-sectional study, consecutive pregnant women with singleton gestations and cervical lengths  $\geq 25$  mm evaluated at the Center for Advanced Obstetrical Care and

Research (CAOCR) [Perinatology Research Branch of the *Eunice Kennedy Shriver* National Institute of Child Health and Human Development, National Institutes of Health, at Wayne State University School of Medicine and Hutzel Women's Hospital, Detroit MI] were invited to participate. All patients provided written informed consent for ultrasound examination prior to enrollment in research protocols approved by the Institutional Review Boards of the National Institute of Child Health and Human Development, and by the Human Investigation Committee of Wayne State University.

Transvaginal ultrasound was performed using an endocavitary probe (Hitachi 8-4 MHz, HI Vision 9000, Hitachi Medical Corporation, Tokyo, Japan). Cervical length was measured in a sagittal view of the cervix, following the recommendations of Burger et al.<sup>45</sup> and Iams et al.<sup>46</sup>. After the cervical length was measured, elastography evaluation was conducted. Three cervical projections were selected for evaluation: one mid-sagittal at the same level of the cervical length measurement, and two cross-sectional, one at the level of the internal and the other at the level of the external cervical os. The rationale in selecting these three anatomical planes was that the mid sagittal view is necessary for cervical length measurement and to identify the internal and external os, while the cross-sectional planes of the internal and external os were selected to compare well-defined regions of the cervix. In the three planes, the interrogation box for color elastography was adjusted to include the entire cervix.

Continuous oscillatory pressure with the US probe was manually applied to the cervix by the ultrasound operator. The intensity was controlled by the pressure bar displayed in the US monitor, ranging from 0 (no pressure) to 7 (highest pressure) and maintained at an intermediate value of 3. Images with the interrogated area covered with color information were selected for strain quantification. Strain was calculated in two regions of interest (ROI), the endocervical canal and entire cervix, delineated by a geometric tool provided by the US manufacturer for irregular structures with eight points of adjustment (Figure 1). A total of six strain estimations were performed in each patient (each anatomical plane in both regions of interest). As strain cannot be estimated in stored images, all measurements were performed at the time of the US examination. The endocervical canal was manually delineated approximately 1-2 mm outside the acoustic interface between the mucous content and the rest of the cervix. The entire cervix was delineated following the acoustic interface between the cervix and the vaginal walls. Strain calculations of the entire cervix also included strain values from the endocervical canal. Strain values represent the averaged displacement or deformation of tissues within the region of interest among consecutive US frames when oscillatory pressure is applied. Strain calculation is performed by computing changes in velocity of the vertical excursions of the ultrasound scatters within the area of elastography interrogation before and after compression is applied.<sup>19</sup> All velocity differences or gradients within the defined region of interest are then averaged.<sup>47</sup>

Strain values obtained from the endocervical canal and entire cervix were independently plotted for defining their normal distribution overall and by region of interest and anatomical plane. In each, three stiff/soft categories were defined: stiff tissues <25<sup>th</sup> percentile; average stiff/soft tissues between 25<sup>th</sup> and 75<sup>th</sup> percentiles; and soft tissues >75<sup>th</sup> percentile. Agreement in classifying patients using these categories was assessed among a subset of 120 elastography estimations made by two operators. Each operator performed the complete US

examination in 20 women, calculating strain values from the endocervical canal and entire cervix in the sagittal plane and cross-sectional planes of the internal and external cervical os. A total of 6 estimations per patient were performed by each operator. Concordance was assessed in the definition of stiff, average soft/stiff, and soft areas according to the strain reference values for each region of interest and anatomical plane.

### Statistical Analysis

Patients were evaluated only once during pregnancy<sup>48,49</sup>. Normality of strain rate distributions was assessed using the Kolmogorov-Smirnov test and inspection of histograms and quantile-quantile (Q-Q) plots. Because multiple cervical tissue strain measurements were clustered within individual patients, regression analysis was performed using linear mixed models to account for the within-subject correlation. A compound symmetry serial correlation structure was used based on model fit as reflected by the Bayesian Information Criterion (BIC). This structure maintains equal correlation among repeated measures nested within an individual participant rather than allowing it to vary over time. Accordingly, the compound symmetry serial correlation coefficient is also an intra-class correlation coefficient. Region of interest and anatomical plane were modeled as fixed effects to evaluate methodological differences in cervical tissue strain estimation. Selected patient characteristics were additionally included as fixed effects in a multivariable model. Effect modification terms were used to determine whether the relationship between methodological differences in cervical tissue strain estimation varied further as a function of clinical patient characteristics. Gestational age and cervical length were each modeled first as continuous parameters; categorical analogues were used to show trend more clearly in constructed figures.

Interoperator agreement for soft, average and stiff tissue strain classifications was assessed using the Kappa-Cohen statistic. *A priori* interpretation of the kappa statistic was based on the following distribution: poor 0.00-0.20; fair 0.21-0.40; moderate 0.41-0.60; substantial 0.61-0.80; and near perfect 0.81-1.00<sup>50</sup>. Percent agreement was also reported. Additionally, the Pearson correlation coefficient is calculated to assess inter-observer correlation between the two operators' strain rate measurements rounded to the nearest tenth decimal place. Rounded measurements were evaluated to represent potentially clinically meaningful differences rather than smaller variations in measurements. Statistical analyses were performed with Med Calc version 9.0.1.0 (Mariakerke, Belgium) and SAS version 9.3 (Cary, North Carolina U.S.) statistical software.

### Results

Cervical elastography was possible in all cases (n=262). A total of 1572 regions of interest for strain evaluation were performed; however, in 15 of them (1%) the strain calculation function was not activated, leaving a total of 1552 elastography estimates for analysis. Patient characteristics are presented in Table 1. Figure 2 shows the distribution of strain values obtained for both regions of interest by anatomical plane (sagittal, internal os, external os). One-way analysis of variance revealed that the distribution of strain rates

differed significantly ( $p < .0001$ ) both by region of interest and separately by anatomical plane for measures obtained within each region of interest.

Data obtained from the endocervical canal and complete cervix, analyzed using a multivariable model, showed: predicted mean strain rates differed significantly by region of interest ( $p < .0001$ ), anatomical plane ( $p < .0001$ ), combined parity and prior preterm delivery ( $p < .0001$ ), gestational length ( $p < .0001$ ) and cervical length ( $p < .01$ ). While gestational age and cervical length are known to be correlated, both were included in the same multivariable model based on a negligible variance inflation factor (1.1) and examination of model fit. Maternal age was marginally associated with cervical tissue strain ( $p = 0.06$ ), although its inclusion as a fixed effect meaningfully reduced model fit, so it was removed from the final model. Further significant differences in estimated mean cervical tissue strain by anatomical plane were found separately as a function of region of interest ( $p < .0001$ ), gestational length ( $p = 0.02$ ) and cervical length ( $p < .01$ ). Together, this final multivariable model explained 60% of the total variation in cervical strain rates. The intra-class correlation coefficient estimated by the compound symmetry serial correlation parameter was 0.33.

Figure 3 shows the predicted mean strain rates for each region of interest by anatomical plane viewed separately as a function of gestational age and cervical length, adjusted further for combined parity and prior preterm delivery. Predicted mean strain rates varied significantly by region of interest and anatomical plane. Holding other factors constant, strain rates measured in the endocervical canal were on average 33% greater than measures obtained in the entire cervix ( $p < .0001$ ). Endocervical strain values obtained in the cross sectional plane of the external cervical os, and in the sagittal plane were 45% and 13% greater when compared to those obtained in the cross sectional plane of the internal cervical os, respectively (both  $p < .0001$ ).

Additional differences were observed by selected patient characteristics. Holding other factors constant, mean strain rate was 14% and 5% greater among multiparous women with a history of preterm delivery and multiparous women without a history of preterm delivery, each compared to nulliparous women ( $p < .01$ ,  $p = 0.06$ , respectively). Among multiparous women, the estimated strain rate was marginally greater in women with a history of preterm delivery compared to those without ( $p = 0.06$ ). Interestingly, apart from modifying the relationship between anatomical plane and tissue strain, continuous gestational length modeled as an independent fixed effect was not significantly associated with cervical tissue strain ( $p = 0.40$ ) and was only marginally associated when cervical length was removed from the adjusted model ( $p = 0.07$ ). Alternatively, cervical length, apart from its modifying relationship with the anatomical plane, was strongly associated with cervical tissue strain, regardless of the inclusion of gestational age in the model ( $p < .01$ ); for each 10 mm unit increase in cervical length, the estimated strain rate decreased by .03, holding other parameters constant.

Overall, the adjusted mean strain rate in women with a cervical length  $< 30$ mm ( $n = 37$ ) was 13% greater than in women with cervical lengths above 30mm ( $p = 0.003$ ). Figure 4 shows the adjusted relationship between categorical cervical length and estimated tissue strain. Women with cervical lengths  $< 30$ mm had significantly softer tissue than women with

cervical lengths at or above 30mm, although correction for multiple pairwise comparisons left only the difference between groups having the shortest (<30) and longest (>45mm) cervical lengths statistically significant. There were no significant differences in adjusted strain rates comparing groups categorized by cervical lengths above 30mm (uncorrected  $p=0.44$ ).

Table 2 shows the inter-observer reliability of two operators' classifications of 120 strain measurements obtained from 20 patients as stiff (strain rate <25<sup>th</sup> percentile), average (25<sup>th</sup>-<75<sup>th</sup> percentile) and soft (>75<sup>th</sup> percentile) tissue, both overall and within each anatomical plane and region. Overall, moderate interobserver agreement in classifying the degree of cervical tissue strain was observed (Kappa =0.43). The two raters agreed exactly on 65% of the three-level cervical tissue strain classifications. Excluding average tissue strain estimations, the operators exhibited substantial overall agreement on soft/stiff estimates (Kappa=0.75), matching on 82% of these classifications. An appreciable overall interobserver correlation for strain measurements rounded to the nearest 10<sup>th</sup> decimal place was also observed (Pearson correlation coefficient 0.73).

The degree of interobserver agreement for soft, average, stiff tissue strain classifications and correlation for rounded strain estimates varied greatly by method of measurement. Substantial interobserver agreement (Kappa=0.67) was achieved specific to measurements obtained in the complete cervix in the cross sectional plane of the internal cervical os; the two operators agreed on 80% of these tissue strain classifications. Alternatively, only fair agreement (Kappa=0.26) was achieved for classifications of measurements obtained in the endocervical canal in the cross sectional plane of the external cervical os; the confidence interval crossing '0' also indicated that the null hypothesis (chance finding) cannot be ruled out with 95% certainty. Similarly, interobserver correlation observed for rounded strain estimates was greatest in both regions of interest for measurements obtained in the cross sectional plane of the internal os as and least for measurements obtained in the sagittal anatomical plane as shown in Figure 5. Altogether, interobserver agreement/correlation was stronger for measurements obtained in the cross sectional plane of the internal os.

## Discussion

### Principal findings of the study

1) ultrasound-derived elastography is capable of measuring differences in softness/stiffness of the uterine cervix, quantified as strain, throughout pregnancy and across selected patient groupings; 2) tissue strain estimates varied systematically by region of interest and anatomical plane adjusted for other sources of variation. In general, measurements from the endocervical canal were on average 33% greater than those obtained in the entire cervix. Endocervical strain values obtained in the cross-sectional plane of the external cervical os, and sagittal plane were 4% and 13% greater compared to those measured in the cross-sectional plane of the internal cervical os, respectively; 3) estimated cervical tissue strain differed significantly by selected patient characteristics- holding other factors constant, mean strain rate was 14% and 5% greater among multiparous women with and without a history of preterm delivery compared to nulliparous women, and was on average 13% greater among women with a cervical length between 25-30mm compared those having



cervical lengths >30 mm. Finally, cervical tissue strain was more strongly associated with cervical length than to gestational age at examination, adjusted for other parameters.

### Physiological cervical changes during pregnancy and elastography

Our results show a continuous reduction in cervical stiffness with decreasing cervical length and advancing gestational age mainly manifested in the internal cervical os. This is in keeping with previous reports showing physiologic changes in the cervix during pregnancy, leading to reduced stiffness and enhanced tensile “capacity”<sup>51,52</sup>. These changes have been attributed to active remodeling of the extracellular matrix (i.e. collagen)<sup>35,53-57</sup>, and to an increase in water content related to increased concentrations of hydrophilic glycosaminoglycans<sup>35,58-60</sup>. Specifically, hyaluronan (HA) has been implicated in the biophysical changes associated with cervical ripening and remodeling<sup>55,61-64</sup>. An increase in water content appears to be a major contributor in the reduction of cervical stiffness throughout pregnancy. The role of other mechanisms (such as the changes in other components of extracellular matrix and smooth muscle) cannot be excluded<sup>38,53,65</sup>.

Increased strain in parous women can be related to changes in the collagen content after pregnancy. Sundtoft et al. sequentially evaluated collagen concentration in the human cervix after delivery, and found that at 9 months the collagen concentration reached 62% (SD 4.45) of dry weight of tissue with no further changes.<sup>64</sup> In addition, Oxlund et al.<sup>66</sup> reported similar mean collagen values in non-pregnant parous women, with a significant reduction in collagen concentration of 1.7% per each previous pregnancy. Cervical strain changes related to a previous preterm delivery might also be related to differences in collagen content. Petersen et al.<sup>67</sup> showed a reduction in the collagen and hydroxyproline concentrations in the cervix of women with history of cervical insufficiency. Contrary, Oxlund et al.<sup>68</sup> could not replicate those results and found no differences in the collagen concentrations of non-pregnant parous women when compared with non-pregnant women with history of cervical insufficiency. Other variables such as changes in the water content, composition of the collagen network and the extracellular matrix in the cervix of pregnant women with history of previous preterm pregnancies might be responsible for the observed increased strain values.

### Factors affecting US elastography evaluation

Graphic representation and averaged values of strain are based on the Young's modulus calculation<sup>69,70</sup>, which is defined as the ratio of uniaxial stress over uniaxial strain<sup>71</sup>. Young's modulus and its graphic representation of displacement are affected by the intensity and direction of the pressure exerted. It is noteworthy, however, that pressure does not affect only the uniaxial components of the Young's modulus but its color graphic representation<sup>72-76</sup>. Therefore, it is important to maintain the same pressure to obtain reproducible results. Both methods perform more efficiently in areas located under the ultrasound beam<sup>77</sup>. Regions located deeper and laterally may not show strain values in agreement with real tissue stiffness. These technical factors might affect the strain rate values when larger regions of interest, such as the entire cervix, are evaluated

The pressure level bar attempts to standardize the stress applied by the operator. Some elastography studies have been performed using an automated device called Fibroscan®, consisting of an US transducer mounted in a mechanic piston which regulates the frequency and intensity of compression<sup>78</sup>. Fibroscan® elastography has been used mainly for detecting focal or diffuse liver disease<sup>79-82</sup>. Unfortunately, an equivalent device is not yet available for obstetrical and gynecological applications. Therefore, the pressure bar must be kept at the same value; otherwise, different pressures may alter strain rate values.

Lack of definition of the cervical boundaries in the ultrasound images might affect the delineation of the entire cervix<sup>83,84</sup>. The area between the anterior border of the cervix and the vaginal wall is technically difficult to delineate, as there is no clearly visible US interphase in all pregnant women<sup>85</sup>. In addition, mechanical pressure applied by the ultrasound probe and bladder size can modify the shape of the cervix<sup>86</sup>, and the software used to perform elastography does not allow multiple adjustments on the contour of the region of interest. Similarly, the force generated by mechanical compression may not reach deep areas of the cervix. This view is consistent with the observation that structures located directly under the ultrasound probe had a high strain rate<sup>87</sup>. All these factors may increase variability among operators, mainly when large areas are assessed. Nevertheless, our results showed a substantial agreement in correctly classifying soft or stiff tissues<sup>50</sup>. We also found that in both regions of interest, measures obtained in the cross-sectional plane of the internal cervical os were more reliable than when obtained otherwise.

### **Clinical application of elastography in Obstetrics and Gynecology**

Elastography is not a new technique; yet, few reports have addressed its use in obstetrics and gynecology<sup>11-17</sup>. To date, elastography has been used to characterize malignant cervical lesions in postmenopausal women<sup>15</sup>, assess stiffness in uterine fibroids compared with the surrounding myometrium in non-pregnant women<sup>11</sup>, and evaluate tissue differences in the presence of subchorionic hematomas<sup>17</sup>. Others have suggested that elastography might help in differentiating between polyps and leiomyomas<sup>18</sup>, that it could be useful for cervical evaluation during pregnancy<sup>14</sup>, and that qualitative assessment of the softness of the cervical canal by elastography might help to predict successful induction of labor<sup>13</sup>.

Recently, Molina et al.<sup>12</sup> evaluated the reproducibility of cervical elastography during pregnancy. Despite reporting acceptable agreement, the authors concluded that it is premature to suggest that elastography can reliably reflect changes associated with cervical ripening. We agree with the authors that such studies need to be conducted. We provide herein a systematic protocol for image acquisition, application of pressure, and placement of the region of interest box to standardize a technique that has been largely subjective thus far. However, we also demonstrate that ultrasound-derived elastography is capable of detecting significant differences in tissue strain by selected patient characteristics, notably including cervical length, combined parity and prior preterm delivery and gestational length at examination. These findings suggest that ultrasound-derived elastography may be able to identify meaningful changes in tissue strain associated with cervical ripening. However, as our study is cross-sectional, longitudinal evaluations are necessary to demonstrate within-



subject change over time associated with cervical ripening and its relationship with clinical outcomes.

## Conclusion

Changes in softness/stiffness of the uterine cervix throughout pregnancy, quantified as strain, can be measured using ultrasound-derived elastography. Cervical tissue strain rates vary both by method of ascertainment and selected patient characteristics. Strain estimation performed in the cross-sectional plane of the internal cervical os may be the most reliable.

## Acknowledgments

This research was supported (in part) by the Perinatology Research Branch, Division of Intramural Research, Eunice Kennedy Shriver National Institute of Child Health and Human Development, NIH, DHHS. The ultrasound experience and technical support of Catherine Ducharme, Denise Haggerty, and Brittany Boven are gratefully acknowledged.

## References

1. Itoh A, Ueno E, Tohno E, Kamma H, Takahashi H, Shiina T, Yamakawa M, Matsumura T. Breast disease: clinical application of US elastography for diagnosis. *Radiology*. 2006; 239:341–50. [PubMed: 16484352]
2. Gheonea IA, Stoica Z, Bondari S. Differential diagnosis of breast lesions using ultrasound elastography. *Indian J Radiol Imaging*. 2011; 21:301–5. [PubMed: 22223946]
3. Garra BS, Cespedes EI, Ophir J, Spratt SR, Zuurbier RA, Magnant CM, Pennanen MF. Elastography of breast lesions: initial clinical results. *Radiology*. 1997; 202:79–86. [PubMed: 8988195]
4. Cespedes I, Ophir J, Ponnekanti H, Maklad N. Elastography: elasticity imaging using ultrasound with application to muscle and breast in vivo. *Ultrasonic Imaging*. 1993; 15:73–88. [PubMed: 8346612]
5. Sebag F, Vaillant-Lombard J, Berbis J, Griset V, Henry JF, Petit P, Oliver C. Shear wave elastography: a new ultrasound imaging mode for the differential diagnosis of benign and malignant thyroid nodules. *J Clin Endocrinol Metab*. 2010; 95:5281–8. [PubMed: 20881263]
6. Bae U, Dighe M, Dubinsky T, Minoshima S, Shamdasani V, Kim Y. Ultrasound thyroid elastography using carotid artery pulsation: preliminary study. *J Ultrasound Med*. 2007; 26:797–805. [PubMed: 17526611]
7. Alam F, Naito K, Horiguchi J, Fukuda H, Tachikake T, Ito K. Accuracy of sonographic elastography in the differential diagnosis of enlarged cervical lymph nodes: comparison with conventional B-mode sonography. *Am J Roentgenol*. 2008; 191:604–10. [PubMed: 18647939]
8. Dudea SM, Giurgiu CR, Dumitriu D, Chiorean A, Ciurea A, Botar-Jid C, Coman I. Value of ultrasound elastography in the diagnosis and management of prostate carcinoma. *Med Ultrason*. 2011; 13:45–53. [PubMed: 21390343]
9. Menten R, Leonard A, Clapuyt P, Vincke P, Nicolae AC, Lebecque P. Transient elastography in patients with cystic fibrosis. *Pediatr Radiol*. 2010; 40:1231–5. [PubMed: 20135110]
10. Gheonea DI, Saftoiu A, Ciurea T, Gorunescu F, Iordache S, Popescu GL, Belciug S, Gorunescu M, Sandulescu L. Real-time sono-elastography in the diagnosis of diffuse liver diseases. *World J Gastroenterol*. 2010; 16:1720–6. [PubMed: 20380003]
11. Ami O, Lamazou F, Mabilie M, Levailant JM, Deffieux X, Frydman R, Musset D. Real-time transvaginal elastosonography of uterine fibroids. *Ultrasound Obstet Gynecol*. 2009; 34:486–8. [PubMed: 19790094]
12. Molina F, Gomez L, Florido J, Padilla M, Nicolaidis KH. Quantification of cervical elastography. A reproducibility study. *Ultrasound Obstet Gynecol*. 2012; 39:685–89. [PubMed: 22173854]
13. Swiatkowska-Freund M, Preis K. Elastography of the uterine cervix: implications for success of induction of labor. *Ultrasound Obstet Gynecol*. 2011; 38:52–6. [PubMed: 21484905]

14. Thomas A. Imaging of the cervix using sonoelastography. *Ultrasound Obstet Gynecol.* 2006; 28:356–7. [PubMed: 16909409]
15. Thomas A, Kummel S, Gemeinhardt O, Fischer T. Real-time sonoelastography of the cervix: tissue elasticity of the normal and abnormal cervix. *Acad Radiol.* 2007; 14:193–200. [PubMed: 17236992]
16. Timmons B, Akins M, Mahendroo M. Cervical remodeling during pregnancy and parturition. *Trends Endocrinol Metab.* 2010; 21:353–61. [PubMed: 20172738]
17. Ogawa M, Nagao D, Mori K, Sato M, Sato A, Shimizu D, Terada Y. Elastography for differentiation of subchorionic hematoma and placenta previa. *Ultrasound Obstet Gynecol.* 2012; 39:112–4. [PubMed: 21728207]
18. Hobson MA, Kiss MZ, Varghese T, Sommer AM, Kliewer MA, Zagzebski JA, Hall TJ, Harter J, Hartenbach EM, Madsen EL. In vitro uterine strain imaging: preliminary results. *J Ultrasound Med.* 2007; 26:899–908. [PubMed: 17592053]
19. Ophir J, Alam SK, Garra B, Kallel F, Konofagou E, Krouskop T, Varghese T. Elastography: ultrasonic estimation and imaging of the elastic properties of tissues. *Proc Inst Mech Eng H.* 1999; 213:203–33. [PubMed: 10420776]
20. Ophir J, Cespedes I, Ponnekanti H, Yazdi Y, Li X. Elastography: a quantitative method for imaging the elasticity of biological tissues. *Ultrason Imaging.* 1991; 13:111–34. [PubMed: 1858217]
21. Parker KJ, Dooley MM, Rubens DJ. Imaging the elastic properties of tissue: the 20 year perspective. *Phys Med Biol.* 2011; 56:R1–R29. [PubMed: 21119234]
22. Wilson LS, Robinson DE, Dadd MJ. Elastography--the movement begins. *Phys Med Biol.* 2000; 45:1409–21. [PubMed: 10870700]
23. Greenleaf JF, Fatemi M, Insana M. Selected methods for imaging elastic properties of biological tissues. *Annu Rev Biomed Eng.* 2003; 5:57–78. [PubMed: 12704084]
24. Gilman G, Khandheria BK, Hagen ME, Abraham TP, Seward JB, Belohlavek M. Strain rate and strain: a step-by-step approach to image and data acquisition. *J Am Soc Echocardiogr.* 2004; 17:1011–20. [PubMed: 15337972]
25. Hall TJ. AAPM/RSNA physics tutorial for residents: topics in US: beyond the basics: elasticity imaging with US. *Radiographics.* 2003; 23:1657–71. [PubMed: 14615571]
26. O'Brien WD Jr. Ultrasound-biophysics mechanisms. *Prog Biophys Mol Biol.* 2007; 93:212–55. [PubMed: 16934858]
27. Cespedes I, Ophir J. Reduction of image noise in elastography. *Ultrasonic Imaging.* 1993; 15:89–102. [PubMed: 8346613]
28. Chaturvedi P, Insana MF, Hall TJ. Ultrasonic and elasticity imaging to model disease-induced changes in soft-tissue structure. *Med Image Anal.* 1998; 2:325–38. [PubMed: 10072200]
29. Dickinson RJ, Hill CR. Measurement of soft tissue motion using correlation between A-scans. *Ultrasound Med Biol.* 1982; 8:263–71. [PubMed: 7101574]
30. Neves LP, Jiang J, Hall TJ, Carneiro AA. Acoustic elastography under dynamic compression using one-dimensional track motion. *Conf Proc IEEE Eng Med Biol Soc.* 2007; 2007:83–6. [PubMed: 18001894]
31. Garra BS. Elastography: current status, future prospects, and making it work for you. *Ultrasound Q.* 2011; 27:177–86. [PubMed: 21873855]
32. Fleury Ede F, Roveda Junior D, Fleury JC, do Carmo Queiroz M, Piato S. Elastography: theory into clinical practice. *Breast J.* 2009; 15:564–6. [PubMed: 19671106]
33. Parikh R, Patel A, Stack T, Socrate S, House M. How the cervix shortens: an anatomic study using 3-dimensional transperineal sonography and image registration in singletons and twins. *J Ultrasound Med.* 2011; 30:1197–204.
34. House M, Socrate S. The cervix as a biomechanical structure. *Ultrasound Obstet Gynecol.* 2006; 28:745–9. [PubMed: 17063451]
35. Myers K, Socrate S, Tzeranis D, House M. Changes in the biochemical constituents and morphologic appearance of the human cervical stroma during pregnancy. *Eur J Obstet Gynecol Reprod Biol.* 2009; 144 Suppl 1:S82–9. [PubMed: 19303693]

36. Mazza E, Nava A, Bauer M, Winter R, Bajka M, Holzapfel GA. Mechanical properties of the human uterine cervix: an in vivo study. *Med Image Anal.* 2006; 10:125–36. [PubMed: 16143559]
37. Myers KM, Paskaleva AP, House M, Socrate S. Mechanical and biochemical properties of human cervical tissue. *Acta Biomater.* 2008; 4:104–16. [PubMed: 17904431]
38. Leppert PC. Anatomy and physiology of cervical ripening. *Clin Obstet Gynecol.* 1995; 38:267–79. [PubMed: 7554594]
39. Allaire AD, D'Andrea N, Truong P, McMahon MJ, Lessey BA. Cervical stroma apoptosis in pregnancy. *Obstet Gynecol.* 2001; 97:399–403. [PubMed: 11239645]
40. Nielsen PE, Howard BC, Crabtree T, Batig AL, Pates JA. The distribution and predictive value of Bishop scores in nulliparas between 37 and 42 weeks gestation. *J Matern Fetal Neonatal Med.* 2012; 25:281–85. [PubMed: 21696336]
41. Bastani P, Hamdi K, Abasalizadeh F, Pourmousa P, Ghatrehsamani F. Transvaginal ultrasonography compared with Bishop score for predicting cesarean section after induction of labor. *Int J Womens Health.* 2011; 3:277–80. [PubMed: 21892338]
42. Eggebo TM, Okland I, Heien C, Gjessing LK, Romundstad P, Salvesen KA. Can ultrasound measurements replace digitally assessed elements of the Bishop score? *Acta Obstet Gynecol Scand.* 2009; 88:325–31. [PubMed: 19172418]
43. Newman RB, Goldenberg RL, Iams JD, Meis PJ, Mercer BM, Moawad AH, Thom E, Miodovnik M, Caritis SN, Dombrowski M. Preterm prediction study: comparison of the cervical score and Bishop score for prediction of spontaneous preterm delivery. *Obstet Gynecol.* 2008; 112:508–15. [PubMed: 18757646]
44. Gomez R, Galasso M, Romero R, Mazor M, Sorokin Y, Goncalves L, Treadwell M. Ultrasonographic examination of the uterine cervix is better than cervical digital examination as a predictor of the likelihood of premature delivery in patients with preterm labor and intact membranes. *Am J Obstet Gynecol.* 1994; 171:956–64. [PubMed: 7943109]
45. Burger M, Weber-Rossler T, Willmann M. Measurement of the pregnant cervix by transvaginal sonography: an interobserver study and new standards to improve the interobserver variability. *Ultrasound Obstet Gynecol.* 1997; 9:188–93. [PubMed: 9165682]
46. Iams JD. Cervical ultrasonography. *Ultrasound Obstet Gynecol.* 1997; 10:156–60. [PubMed: 9339521]
47. Hitachi M. *Real Time Tissue Elastography (Manual).* 2005-2009
48. Bland JM, Altman DG. Applying the right statistics: analyses of measurement studies. *Ultrasound Obstet Gynecol.* 2003; 22:85–93. [PubMed: 12858311]
49. Altman DG, Chitty LS. Design and analysis of studies to derive charts of fetal size. *Ultrasound Obstet Gynecol.* 1993; 3:378–84. [PubMed: 12797237]
50. Landis JR, Koch GG. The measurement of observer agreement for categorical data. *Biometrics.* 1977; 33:159–74. [PubMed: 843571]
51. Read CP, Word RA, Ruscheinsky MA, Timmons BC, Mahendroo MS. Cervical remodeling during pregnancy and parturition: molecular characterization of the softening phase in mice. *Reproduction.* 2007; 134:327–40. [PubMed: 17660242]
52. Winkler M, Rath W. Changes in the cervical extracellular matrix during pregnancy and parturition. *J Perinat Med.* 1999; 27:45–60. [PubMed: 10343934]
53. Minamoto T, Arai K, Hirakawa S, Nagai Y. Immunohistochemical studies on collagen types in the uterine cervix in pregnant and nonpregnant states. *Am J Obstet Gynecol.* 1987; 156:138–44. [PubMed: 3541616]
54. Akins ML, Luby-Phelps K, Bank RA, Mahendroo M. Cervical softening during pregnancy: regulated changes in collagen cross-linking and composition of matricellular proteins in the mouse. *Biol Reprod.* 2011; 84:1053–62. [PubMed: 21248285]
55. House M, Kaplan DL, Socrate S. Relationships between mechanical properties and extracellular matrix constituents of the cervical stroma during pregnancy. *Semin Perinatol.* 2009; 33:300–7. [PubMed: 19796726]
56. Uldbjerg N, Ekman G, Malmstrom A, Olsson K, Ulmsten U. Ripening of the human uterine cervix related to changes in collagen, glycosaminoglycans, and collagenolytic activity. *Am J Obstet Gynecol.* 1983; 147:662–6. [PubMed: 6638110]

57. Kleissl HP, van der Rest M, Naftolin F, Glorieux FH, de Leon A. Collagen changes in the human uterine cervix at parturition. *Am J Obstet Gynecol.* 1978; 130:748–53. [PubMed: 637097]
58. Junqueira LC, Zugaib M, Montes GS, Toledo OM, Krisztan RM, Shigihara KM. Morphologic and histochemical evidence for the occurrence of collagenolysis and for the role of neutrophilic polymorphonuclear leukocytes during cervical dilation. *Am J Obstet Gynecol.* 1980; 138:273–81. [PubMed: 7416217]
59. Osmers R, Rath W, Pflanz MA, Kuhn W, Stuhlsatz HW, Szeverenyi M. Glycosaminoglycans in cervical connective tissue during pregnancy and parturition. *Obstet Gynecol.* 1993; 81:88–92. [PubMed: 8416467]
60. Straach KJ, Shelton JM, Richardson JA, Hascall VC, Mahendroo MS. Regulation of hyaluronan expression during cervical ripening. *Glycobiology.* 2005; 15:55–65. [PubMed: 15317739]
61. Ruschinsky M, De la Motte C, Mahendroo M. Hyaluronan and its binding proteins during cervical ripening and parturition: dynamic changes in size, distribution and temporal sequence. *Matrix biology.* 2008; 27:487–97. [PubMed: 18353623]
62. Uldbjerg N, Malmstrom A. The role of proteoglycans in cervical dilatation. *Semin Perinatol.* 1991; 15:127–32. [PubMed: 1876867]
63. Buhimschi CS, Sora N, Zhao G, Buhimschi IA. Genetic background affects the biomechanical behavior of the postpartum mouse cervix. *Am J Obstet Gynecol.* 2009; 200:434 e1–7. [PubMed: 19200937]
64. Sundtoft I, Sommer S, Uldbjerg N. Cervical collagen concentration within 15 months after delivery. *Am J Obstet Gynecol.* 2011; 205:59 e1–3. [PubMed: 22088899]
65. Burger LL, Sherwood OD. Relaxin increases the accumulation of new epithelial and stromal cells in the rat cervix during the second half of pregnancy. *Endocrinology.* 1998; 139:3984–95. [PubMed: 9724054]
66. Oxlund BS, Ortoft G, Bruel A, Danielsen CC, Bor P, Oxlund H, Uldbjerg N. Collagen concentration and biomechanical properties of samples from the lower uterine cervix in relation to age and parity in non-pregnant women. *Reprod Biol Endocrinol.* 2010; 8:82. [PubMed: 20604933]
67. Petersen LK, Uldbjerg N. Cervical collagen in non-pregnant women with previous cervical incompetence. *Eur J Obstet Gynecol Reprod Biol.* 1996; 67:41–5. [PubMed: 8789748]
68. Oxlund BS, Ortoft G, Bruel A, Danielsen CC, Oxlund H, Uldbjerg N. Cervical collagen and biomechanical strength in non-pregnant women with a history of cervical insufficiency. *Reprod Biol Endocrinol.* 2010; 8:92. [PubMed: 20673361]
69. Varghese T. Quasi-Static Ultrasound Elastography. *Ultrasound Clin.* 2009; 4:323–38. [PubMed: 20798841]
70. McLaughlin JR, Zhang N, Manduca A. Calculating tissue shear modulus and pressure by 2D Log-Elastographic methods. *Inverse Probl.* 2010; 26
71. Garra BS. Imaging and estimation of tissue elasticity by ultrasound. *Ultrasound Q.* 2007; 23:255–68. [PubMed: 18090836]
72. Hoeks AP, Arts TG, Brands PJ, Reneman RS. Comparison of the performance of the RF cross correlation and Doppler autocorrelation technique to estimate the mean velocity of simulated ultrasound signals. *Ultrasound Med Biol.* 1993; 19:727–40. [PubMed: 8134974]
73. Hoeks AP, Brands PJ, Arts TG, Reneman RS. Subsample volume processing of Doppler ultrasound signals. *Ultrasound Med Biol.* 1994; 20:953–65. [PubMed: 7886854]
74. Wells PN. Ultrasonic colour flow imaging. *Phys Med Biol.* 1994; 39:2113–45. [PubMed: 15551544]
75. Kim S, Aglyamov SR, Park S, O'Donnell M, Emelianov SY. An autocorrelation-based method for improvement of sub-pixel displacement estimation in ultrasound strain imaging. *IEEE Trans Ultrason Ferroelectr Freq Control.* 2011; 58:838–43. [PubMed: 21507761]
76. Shamdasani V, Kim Y. Two-dimensional autocorrelation method for ultrasound-based strain estimation. *Conf Proc IEEE Eng Med Biol Soc.* 2004; 2:1380–3. [PubMed: 17271950]
77. Varghese T, Ophir J. The nonstationary strain filter in elastography: Part I. Frequency dependent attenuation. *Ultrasound Med Biol.* 1997; 23:1343–56. [PubMed: 9428134]

78. Malekzadeh R, Poustchi H. Fibroscan for assessing liver fibrosis: An acceptable alternative for liver biopsy: Fibroscan: an acceptable alternative for liver biopsy. *Hepat Mon.* 2011; 11:157–8. [PubMed: 22087136]
79. Degos F, Perez P, Roche B, Mahmoudi A, Asselineau J, Voitot H, Bedossa P. Diagnostic accuracy of FibroScan and comparison to liver fibrosis biomarkers in chronic viral hepatitis: a multicenter prospective study (the FIBROSTIC study). *J Hepatol.* 2010; 53:1013–21. [PubMed: 20850886]
80. Fransen van de Putte D, Blom R, van Soest H, Mundt M, Vermeer C, Arends J, de Knegt RE, Mauser-Bunschoten E, van Erpecum K. Impact of Fibroscan on management of chronic viral hepatitis in clinical practice. *Ann Hepatol.* 2011; 10:469–76. [PubMed: 21911887]
81. Sporea I, Nicolita D, Sirli R, Deleanu A, Tudora A, Bota S. Assessment of noninvasive liver stiffness in inactive HBsAg carriers by transient elastography: Fibroscan in inactive HBsAg carriers. *Hepat Mon.* 2011; 11:182–5. [PubMed: 22087140]
82. Foucher J, Chanteloup E, Vergniol J, Castera L, Le Bail B, Adhoute X, Bertet J, Couzigou P, de Ledinghen V. Diagnosis of cirrhosis by transient elastography (FibroScan): a prospective study. *Gut.* 2006; 55:403–8. [PubMed: 16020491]
83. Rovas L, Sladkevicius P, Strobel E, Valentin L. Intraobserver and interobserver reproducibility of three-dimensional gray-scale and power Doppler ultrasound examinations of the cervix in pregnant women. *Ultrasound Obstet Gynecol.* 2005; 26:132–7. [PubMed: 15959922]
84. Hoesli IM, Surbek DV, Tercanli S, Holzgreve W. Three dimensional volume measurement of the cervix during pregnancy compared to conventional 2D-sonography. *Int J Gynaecol Obstet.* 1999; 64:115–9. [PubMed: 10189018]
85. Bergelin I, Valentin L. Patterns of normal change in cervical length and width during pregnancy in nulliparous women: a prospective, longitudinal ultrasound study. *Ultrasound Obstet Gynecol.* 2001; 18:217–22. [PubMed: 11555449]
86. Bowie JD, Andreotti RF, Rosenberg ER. Sonographic appearance of the uterine cervix in pregnancy: the vertical cervix. *Am J Roentgenol.* 1983; 140:737–40. [PubMed: 6601381]
87. Kallel F, Varghese T, Ophir J, Bilgen M. The nonstationary strain filter in elastography: Part II. Lateral and elevational decorrelation. *Ultrasound Med Biol.* 1997; 23:1357–69. [PubMed: 9428135]



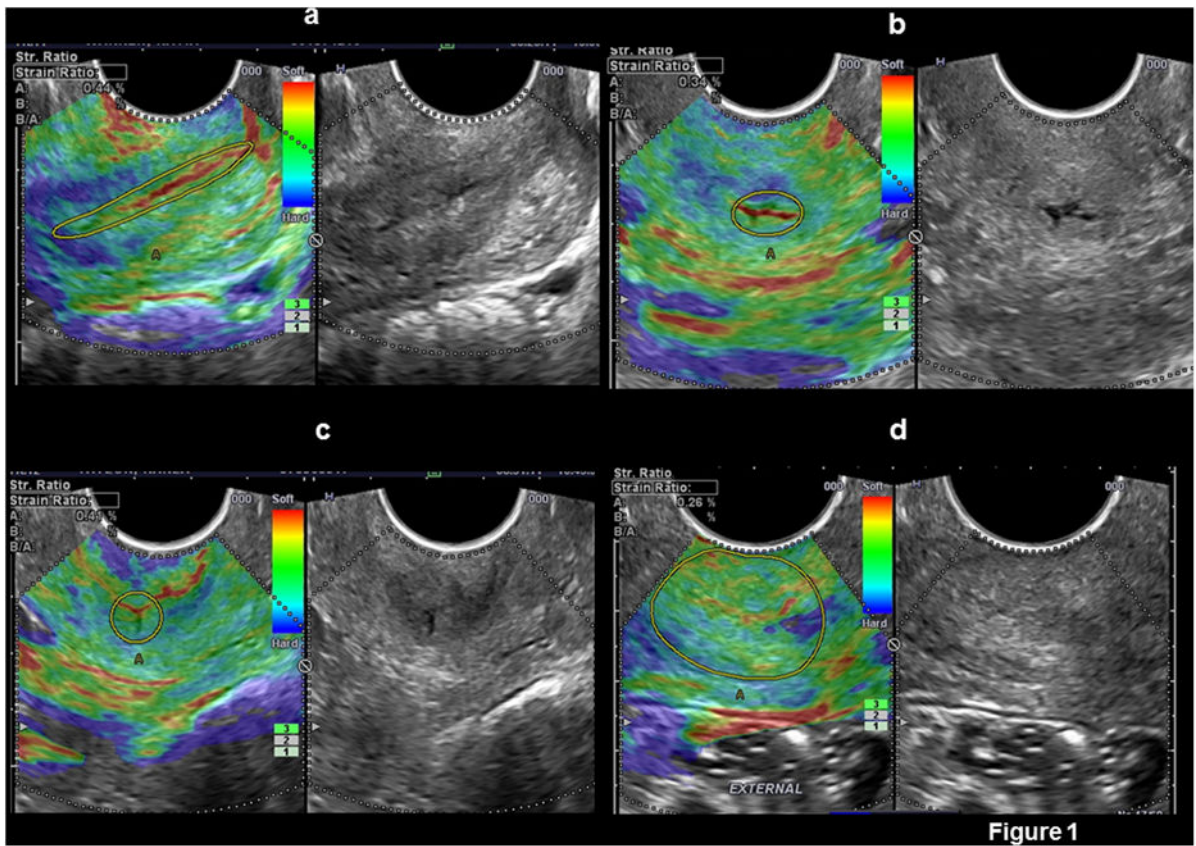
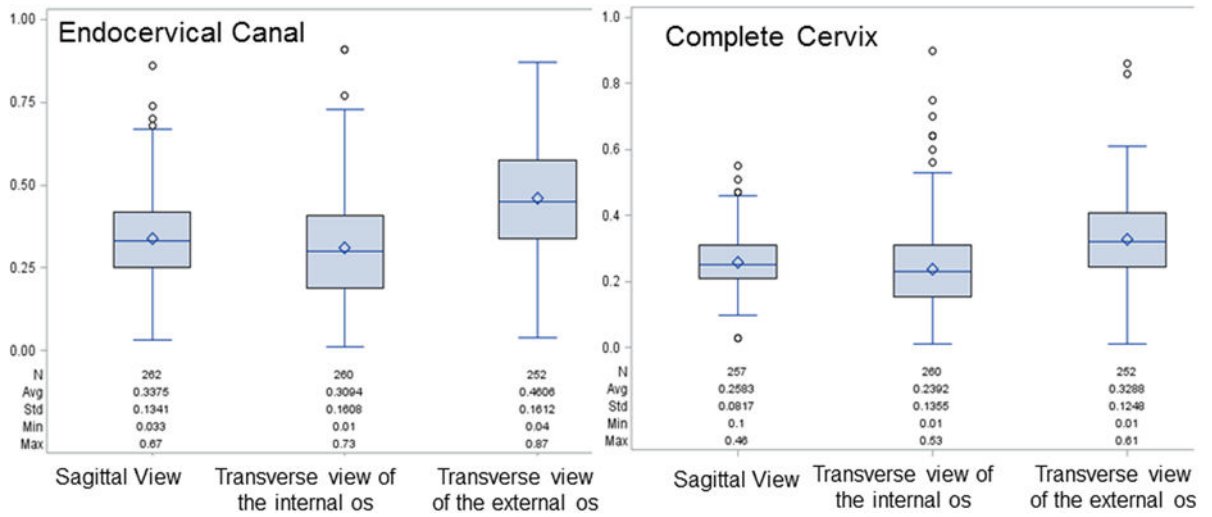


Figure 1

**Figure 1.** Cervical strain calculation performed in: a) endocervical canal in a sagittal plane, b) endocervical canal in a cross sectional plane at the level of the internal os, c) endocervical canal in a cross sectional plane at the level of the external cervical os, and d) complete cervix in a cross sectional plane at the level of the external cervical os.





**Figure 2.** Distribution of strain values obtained from the endocervical canal and entire cervix in the three studied anatomical planes.

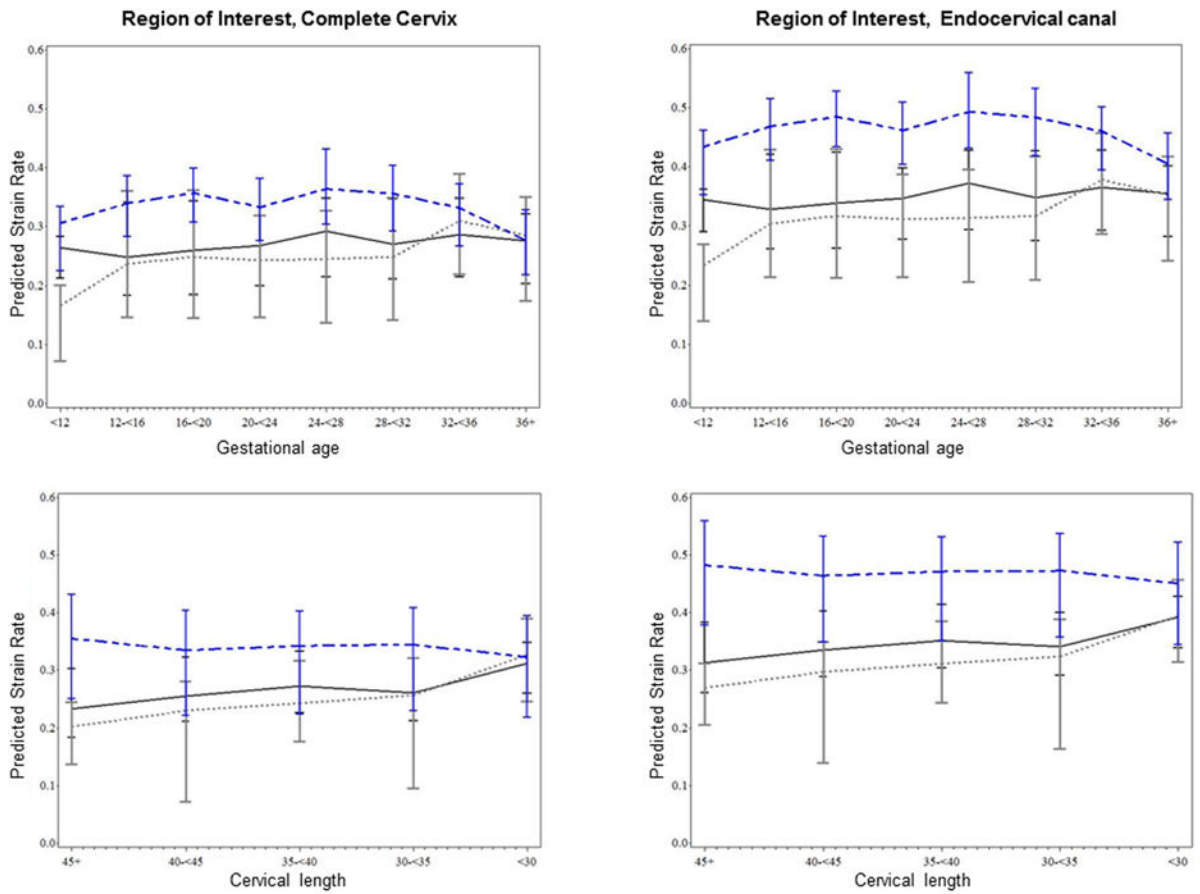


**Figure 3. Estimated cervical tissue strain by region of interest and anatomical view as a function of gestational age and cervical length at assessment, adjusted for combined parity and prior preterm delivery**

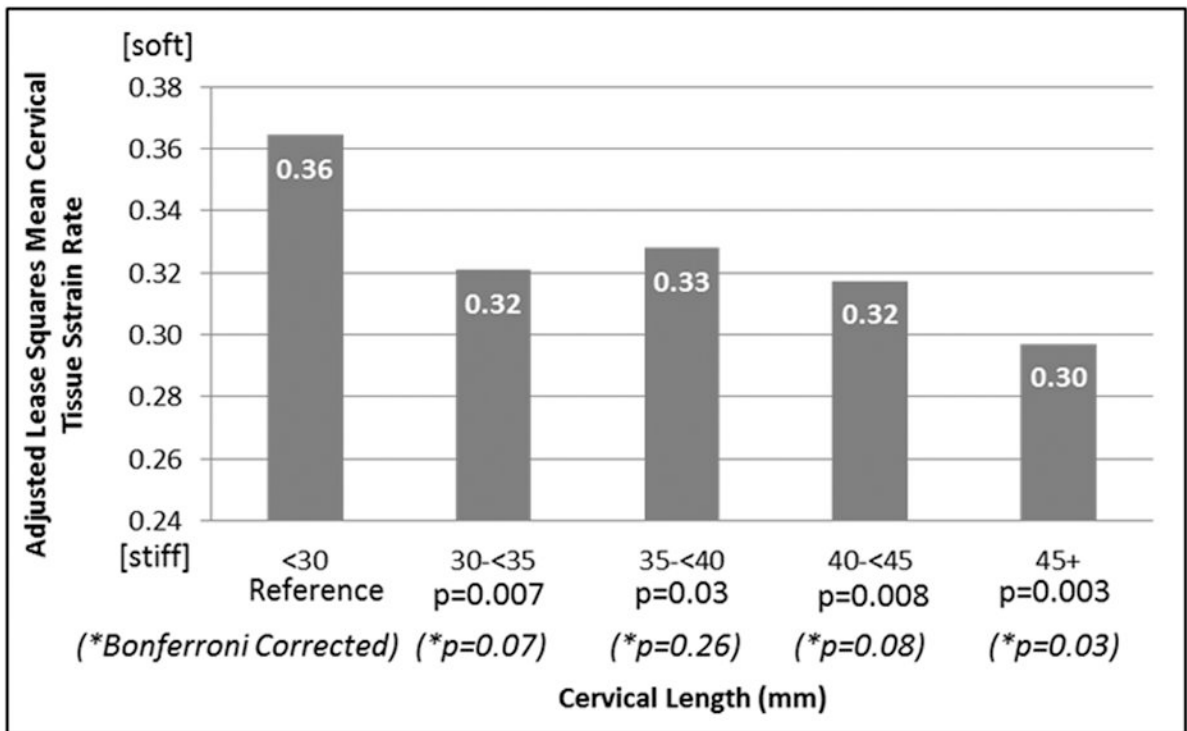
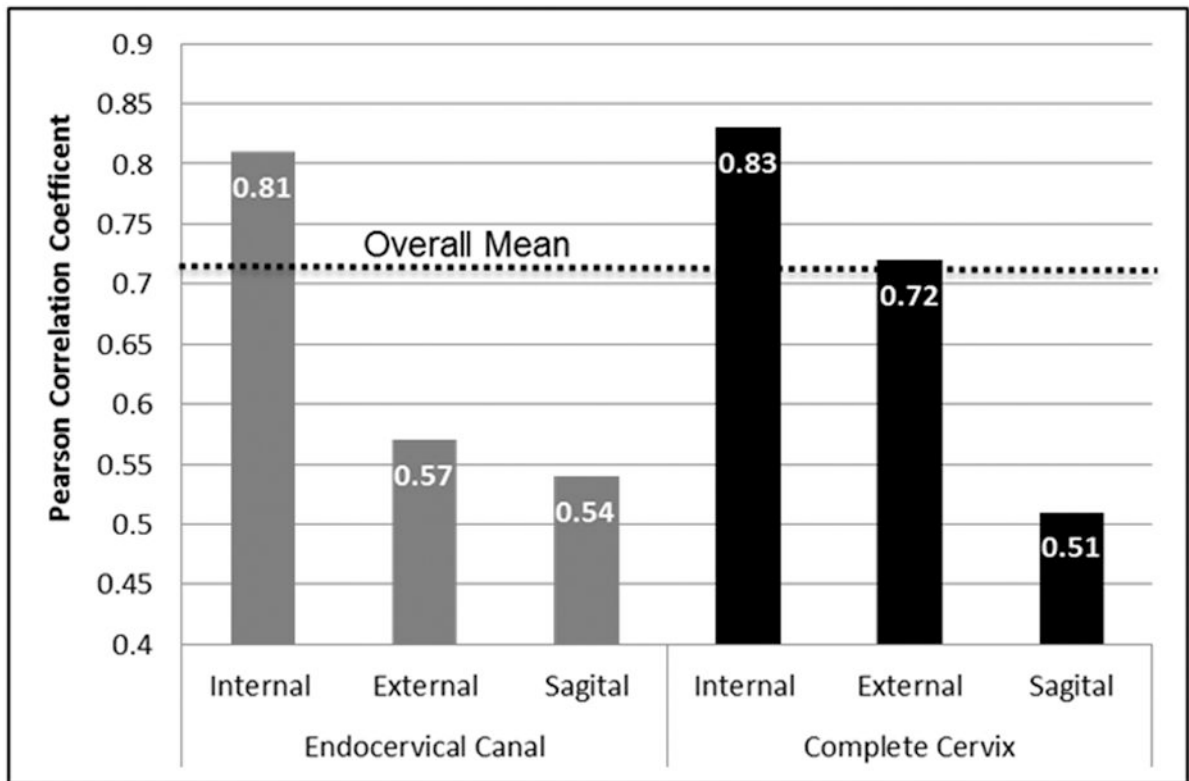


Figure 4. Least squares mean cervical tissue strain rate by categorical cervical length adjusted for measurement differences and combined parity and prior preterm delivery



**Figure 5.** Interobserver correlation for 120 cervical tissue strain estimates rounded to the nearest 10<sup>th</sup> decimal place obtained in a sub-sample of 20 women by region of interest and anatomical plane

**Table 1**  
**Demographics of the studied population**

<b>Maternal characteristics</b>		
Age, completed years, median (range)	23	(17-41)
Number of pregnancies, n, median (range)	1	(1-14)
Gestational age at ultrasound, weeks + days, median (range)	21+ 4	(8+2-40+3)
Cervical length, mm, median (range)	36	(25-52)
Prior preterm delivery, n, (%)	55	(21)

**Table 2**

Interobserver agreement and correlation in classifying and measuring cervical tissue strain in a sub-sample of 20 women (120 measurements- 6 per participant)

Region	View	Simple Kappa		Weighted Kappa		Exact Agreement <sup>^</sup>	Pearson Correlation Coefficient <sup>*</sup>
		Value	95% CI	Value	95% CI		
Endocervical Canal	Internal	0.43	0.09	0.77	0.24	0.87	0.81
	External	0.26	-0.06	0.59	-0.06	0.66	0.83
	Sagittal	0.44	0.13	0.76	0.09	0.78	0.53
Complete Cervix	Internal	0.67	0.39	0.95	0.40	0.97	0.51
	External	0.46	0.10	0.81	0.09	0.83	0.72
	Sagittal	0.32	0.02	0.61	0.01	0.61	0.57
<i>Total</i>		<i>0.43</i>	<i>0.30</i>	<i>0.56</i>	<i>0.32</i>	<i>0.60</i>	<i>0.73</i>

**Note:**

<sup>^</sup> Exact agreement characterizes categorical soft/average/stiff tissue classifications.

<sup>\*</sup> The Pearson correlation coefficient characterizes interobserver correlation for cervical tissue strain measurements rounded to the nearest tenth decimal place.